Journal of The Electrochemical Society, **151** (10) G704-G708 (2004)
0013-4651/2004/151(10)/G704/5/$7.00 © The Electrochemical Society, Inc.

Physical and Barrier Properties of PECVD Amorphous Silicon-Oxycarbide from Trimethylsilane and CO_2

Chiu-Chih Chiang,[a,z] I-Hsiu Ko,[a] Mao-Chieh Chen,[a,*] Zhen-Cheng Wu,[b] Yung-Cheng Lu,[b] Syun-Ming Jang,[b] and Mong-Song Liang[b]

[a]*Department of Electronics Engineering, National Chiao-Tung University, Hsinchu 300, Taiwan*
[b]*Department of Dielectric and CMP, Advanced Module Technology Division, Taiwan Semiconductor Manufacturing Company, Science-Based Industrial Park, Hsinchu, Taiwan*

This work investigates the thermal stability and physical and barrier properties of amorphous silicon-carbide (α-SiC) and amorphous silicon-oxycarbide (α-SiCO) dielectric barriers deposited by plasma-enhanced chemical vapor deposition (PECVD) using trimethylsilane (3MS) precursor and He carrier gas. Films were deposited without and with various CO_2 flow rates. The dielectric constant of the α-SiCO films decreased with increasing CO_2 flow rate. Increasing CO_2 flow rate also promotes better thermal stability, higher breakdown field, lower leakage current, and superior resistance to Cu diffusion through the films. The improved barrier property is attributed to the denser and less porous structure of the α-SiCO dielectric barrier upon CO_2 addition. The α-SiCO barrier films deposited with the large (1200 sccm) CO_2 flow rate exhibit the low k value of 3.7, thermal stability up to 550°C, room-temperature breakdown field of 8 MV/cm and leakage current densities of 10^{-7} to 10^{-6} A/cm^2 at 3 MV/cm, and a superb Cu barrier property.
© 2004 The Electrochemical Society. [DOI: 10.1149/1.1790510] All rights reserved.

Manuscript submitted September 11, 2003; revised manuscript received March 2, 2004. Available electronically September 27, 2004.

To reduce the interconnect resistance-capacitance (RC) time-delay, a dominant factor in determining the performance of ultralarge scale integrated (ULSI) circuits, it is inevitable to use copper (Cu) metal to replace aluminum (Al) and its alloys in integrated circuits as the multilevel interconnect material and low dielectric constant (low-k) dielectric materials instead of the conventional SiO_2 film. Cu is the most suitable interconnect metal because of its low electrical resistivity and excellent electromigration resistance, and the use of low-k materials as the inter- and intra-layer dielectrics (ILD) can reduce the signal-propagation delay, crosstalk-noise between metal lines, and power dissipation of integrated circuits. While many low-k ($k < 3$) dielectric materials have been used as ILDs, high dielectric constant ($k > 7$) silicon nitride is still the primary candidate for the Cu cap-barrier and etching stop layer required in the Cu damascene structure. It is desirable to replace silicon nitride with dielectric materials of lower k value ($k < 5$) to further reduce the effective dielectric constant of the Cu interconnect system. In recent years, amorphous silicon-carbide (α-SiC) and amorphous silicon-nitricarbide (α-SiCN) deposited by plasma-enhanced chemical vapor deposition (PECVD) using organosilicate gases are receiving extensive attention for applications as Cu cap-barrier and etching stop layer in Cu damascene structures because of their lower k value, better etching selectivity with respect to organosilicate glass (OSG), excellent chemical mechanical polishing (CMP) strength, and superb property as Cu barrier and passivation layer in terms of electromigration resistance and Cu hillock density.[1,2] There are studies on 3MS-based α-SiC and α-SiCN barriers which show k values in the range of 4 to 5,[1-5] while the α-SiCO barriers deposited using tetramethylsilane (4MS), hexamethydisiloxane (HMDSO) or trimethoxysilane (TMOS) precursor exhibit an even lower k value of 3.9.[6-8] Moreover, it has been reported that the α-SiCO barrier film deposited using 3MS precursor and He carrier gas with an addition of O_2 exhibits a k value of 3.7 under an optimal process condition.[9] In this work, we investigated the thermal stability and physical and barrier properties for four α-SiC and α-SiCO dielectric barrier films, with dielectric constants between 3.7 and 4.4, deposited using trimethylsilane (3MS) precursor and He carrier gas with various CO_2 flow rates.

* Electrochemical Society Active Member.
[z] E-mail: ccchiang.ee88g@nctu.edu.tw

Experimental

Four α-SiC(O) dielectric barrier films were deposited using 3MS $[(CH_3)_3SiH]$ precursor and He carrier gas with various CO_2 flow rates. The resulting films were investigated with respect to their thermal stability and physical and barrier properties. In this study, all of the α-SiC(O) films were deposited to a thickness of 50 nm on p-type, (100)-oriented Si wafers at a temperature of 300-400°C, a gas pressure of 1-5 Torr, and a plasma power of 100-300 W using a parallel-plate PECVD system operated at 13.56 MHz. The flow rate ratio of 3MS/He gases was maintained at 2/5, while the flow rate of CO_2 was separately controlled at 0, 300, 600, and 1200 sccm, which resulted in four α-SiC(O) films with different elemental compositions. All films were thermally annealed at 400°C for 30 min in N_2 ambient to remove moisture possibly absorbed in the dielectric prior to the investigation of the films' physical properties or the deposition of the electrode (TaN/Cu or Al) to construct the metal-insulator-semiconductor (MIS) capacitor structure. For the construction of TaN/Cu-electrode MIS capacitors, a Cu layer of 200 nm thickness was sputter-deposited on the α-SiC(O) dielectric films using a dc magnetron sputtering system was followed by the reactive sputter deposition of a 50 nm thick TaN layer on the Cu surface in the same sputtering system without breaking the vacuum. The TaN film served as a passivation layer to prevent the Cu electrode from oxidation in the subsequent high-temperature processes. For a comparison, Al-electrode control samples were also prepared by depositing a 500 nm thick Al layer directly on the α-SiC(O) dielectric surfaces using a thermal evaporation system. All metal electrodes with a circular area and 0.84 mm diam were defined by a lift-off process to prevent unexpected deterioration of the dielectric films by wet chemical etching. To ensure good contact in electrical measurements, a 500 nm thick Al layer was also thermally evaporated on the back surface of the Si substrate for all samples. Some of the completed MIS samples were thermally annealed at 400°C for 30 min in N_2 ambient. This annealing step eliminates the plasma-induced damage during the sputter deposition of the TaN/Cu electrodes and also provides the driving force for Cu diffusion.

An HP4145B semiconductor parameter analyzer was used to measure the dielectric leakage current and provide the bias for the bias-temperature-stress (BTS) test. Auger electron spectroscopy (AES) was used to detect the elemental compositions of the dielectric barrier films. Fourier transform infrared spectroscopy (FTIR, ASTeX PDS-17 system) was used to analyze the chemical bonding of the dielectrics from 600 to 2300 cm^{-1} wavenumber. The film thickness and refractive index were measured using a well-

Downloaded on 2014-04-27 to IP 140.113.38.11 address. Redistribution subject to ECS terms of use (see ecsdl.org/site/terms_use) unless CC License in place (see abstract).

Table I. Properties of 3MS-based α-SiC(O) dielectric films studied in this work.

Sample ID	SCO0	SCO3	SCO6	SCO12
CO_2 flow rate (sccm)	0	300	600	1200
Elemental composition				
Si (%)	51	45	40	38
C (%)	47	42	38	37
O (%)	2	13	22	25
Structure	α-SiC	α-SiCO	α-SiCO	α-SiCO
Refractive index @ 633 nm	2.04	1.94	1.76	1.72
Electronic *k*-value	4.16	3.76	3.09	2.95
k-value @ 1 MHz	4.41	4.06	3.81	3.73
Ionic and dipolar *k*-value	0.25	0.30	0.72	0.78

calibrated n&k analyzer at 633 nm wavelength, and the *k* value of the dielectrics was determined by the maximum capacitance of the Al-gated MIS capacitors measured at 1 MHz using a Keithley 82 C-V measurement system. The film density was directly calculated by the ratio of mass to volume of the film, whereas the film mass was measured by an electronic balance and the film volume was calculated from the film thickness and the area of the substrate wafer.

Results and Discussion

Physical properties and thermal stability.—Table I shows the properties of the four 3MS-based α-SiC(O) dielectric barrier films studied in this work. It is found that the oxygen content of the dielectrics, as determined by AES, increases with increasing CO_2 flow rate. Notably, the C/Si concentration ratio remains nearly constant at 0.92 to 0.97 for all four films. However, the refractive index of the dielectrics decreases with increasing CO_2 flow rate, and thus with increasing oxygen content. This is consistent with previous results reported in the literature for α-SiC(O) films deposited using O_2/3MS, N_2O/HMDSO, O_2/4MS, and N_2O/4MS gases.[9-12] The *k* value at 1 MHz consists of three components arising from the contribution of electronic, ionic, and dipolar *k* value,[9,10,13,14]

$$k\ (\text{at 1 MHz}) = k_e + k_{ion} + k_{dipolar} \quad [1]$$

The electronic contribution arises from the displacement of the electrons relative to a nucleus. The ionic contribution comes from the displacement of the charged ion cores of the atoms with respect to other ions, and the dipolar contribution arises from the change of orientation for the molecules with a permanent electric dipole moment in an applied electric field. The electronic *k*-value (k_e), which equals the square of refractive index,[9,10,13,14] and the *k* value (at 1 MHz) of the film both decrease with increasing CO_2 flow rate. However, the ionic and dipolar *k* value, which is obtained by subtracting k_e from the *k*-value at 1 MHz,[9,10,13] increases with increasing CO_2 flow rate. This reduction in the electronic contribution to *k* value with increasing CO_2 flow rate is attributed to the increase in the density of the Si-O bonds in the film,[9,10] which is more ionic and polarizable than the Si-C bond.[9,10,14,15] Thus, *k* value for an α-SiC(O) film (at 1 MHz), which is dominated by the electronic polarization, would decrease with increasing incorporation of oxygen.[9,12] The higher electronegativity of the oxygen atom also decreases the polarizability of bonds and results in a lower *k* value of film.[9] The change of oxygen concentration, refractive index, and *k* value (at 1 MHz) for the α-SiC(O) dielectric films with increasing CO_2 flow rate appear to saturate when the CO_2 flow rate was increased from 600 to 1200 sccm. Table II shows the chemical composition, density, and porosity of the four films. The chemical composition was determined from the AES analysis, while the porosity was calculated from the film density and molecular weight of each film.[15] It is conceivable that the α-SiC(O) dielectric films with a less dense and highly porous structure may exhibit poor thermal stability and poor electrical and barrier properties.[16]

Figure 1 shows the FTIR spectra of the α-SiC(O) dielectric films before and after thermal annealing at various temperatures (30 min in N_2 ambient). It is notable that the decreasing peak at 1100 cm^{-1} (*i.e.*, going below the background) resulted from the bare Si reference wafer calibrated by the FTIR measurement system. By introducing the CO_2 gas in the deposition process, we found that the absorbance of the combined Si-C stretching and Si-CH_3 rocking/wagging modes (800 cm^{-1})[9,11] and the Si-H stretching mode (2100 cm^{-1}) decreased, whereas the absorbance near 1000 cm^{-1} significantly increased (Fig. 1a and b). The peak near 1000 cm^{-1} represents the Si-$(CH_2)_n$ bending/wagging (995 cm^{-1}) for α-SiC films or Si-O stretching (1006 cm^{-1}) for α-SiCO films,[9] and the Si-$(CH_2)_n$ absorption for α-SiC films vanishes after thermal annealing at 600°C. Specifically, the FTIR spectra of the SCO6 and SCO12 films are similar in every respect; this implies that the CO_2 gas flow rates larger than 1200 sccm would produce little change in the film properties.

The Si-H stretching (2100 cm^{-1}) and Si-CH_3 bending (1250 cm^{-1}) absorptions in the films decrease after thermal annealing at temperatures above 500°C, as shown in Fig. 2. In Fig. 2, the spectra have been shifted for clarity. Chemical desorption of carbon- and hydrogen-related groups were detected at temperatures above 550°C for the SCO0 and SCO3 films and at 600°C for the SCO6 and SCO12 films. Figure 3 shows the thickness shrinkage, refractive index, and dielectric constant as a function of the annealing temperature for the α-SiC(O) barrier films. The film thickness remained nearly constant for all films at temperatures up to 450°C. However, all films started to show shrinkage at 500°C. The SCO0 and SCO3 films shrank more than 5% at 550°C and more than 10% at 600°C, presumably due to desorption of hydrocarbon groups (Fig. 2). Similarly, shrinkage of more than 5% was observed at 600°C for the SCO6 and SCO12 films. The outgassing implies that changes in chemical bonding structure and physical microstructure of the dielectric film occur, resulting in the variation of refractive index and dielectric constant (Fig. 3b and c). In summary, the 3MS-based α-SiCO dielectric barrier films deposited with a higher CO_2 flow rate ($\geqslant$600 sccm) are stable up to 550°C, while the films deposited without or with lower CO_2 flow rates ($\leqslant$300 sccm) are stable up to 500°C. Interestingly, the α-SiC(O) dielectric barrier film with a lower dielectric constant exhibits a higher thermal stability-temperature in this study, which is contrary to the α-SiC and α-SiCN dielectric barrier films investigated in our other work.[17,18]

Table II. Chemical composition, density, and porosity of 3MS-based α-SiC(O) dielectrics and SiO_2 films.

Sample ID	SCO0	SCO3	SCO6	SCO12	Oxide
Chemical composition	$SiC_{0.92}O_{0.04}$	$SiC_{0.93}O_{0.29}$	$SiC_{0.95}O_{0.55}$	$SiC_{0.97}O_{0.66}$	SiO_2
Density (g/cm^3)	1.24	1.43	1.65	1.80	2.20
Porosity (%)[a]	14.77	10.96	6.64	2.21	0

[a] Porosity (%) is calculated from the film density (ρ) and molar weight (M) of α-SiC(O) dielectric, based on the assumption that the oxide (SiO_2) has no porosity; thus $(1 - \text{porosity})M_{SCO}/M_{oxide} = \rho_{SCO}/\rho_{oxide}$.

Downloaded on 2014-04-27 to IP 140.113.38.11 address. Redistribution subject to ECS terms of use (see ecsdl.org/site/terms_use) unless CC License in place (see abstract).

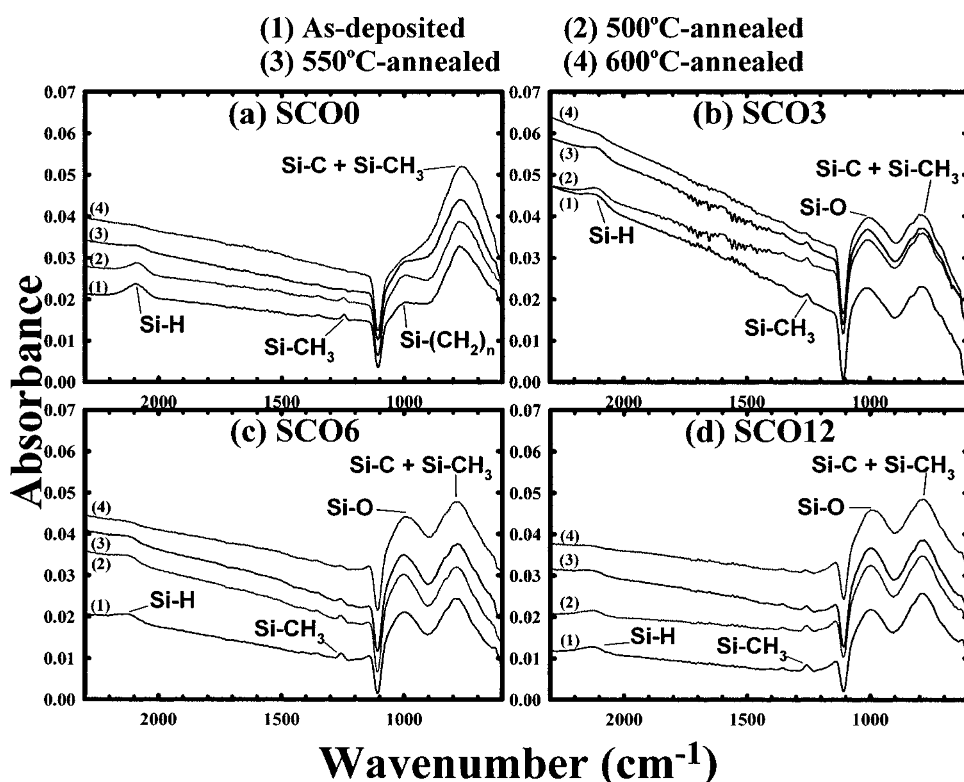

Figure 1. FTIR spectra of (a) SCO0, (b) SCO3, (c) SCO6, and (d) SCO12 dielectric films before and after thermal annealing at various temperatures (30 min in N_2 ambient).

Electrical and barrier properties.—Figure 4 shows the room-temperature leakage current density for the 400°C annealed MIS capacitors with Al gates made using α-SiC(O) films deposited with different CO_2 flow rates. The measurements were performed with the MIS capacitors biased in the accumulation region. The breakdown field is defined as the field strength such that the leakage current of the MIS capacitor reaches 20 mA (equivalent to 3.57 A/cm^2). The breakdown field of the α-SiC(O) films increases with increasing CO_2 flow rate. A similar result was observed in the α-SiC(O) dielectric films deposited using O_2/3MS gases of various flow ratios and the breakdown field increased with increasing O_2 flow rates.[9] Figure 5 shows the room-temperature leakage current density for the as-fabricated as well as annealed (30 min in N_2 ambient at 400°C) TaN/Cu-gated MIS capacitors with α-SiC(O) di-

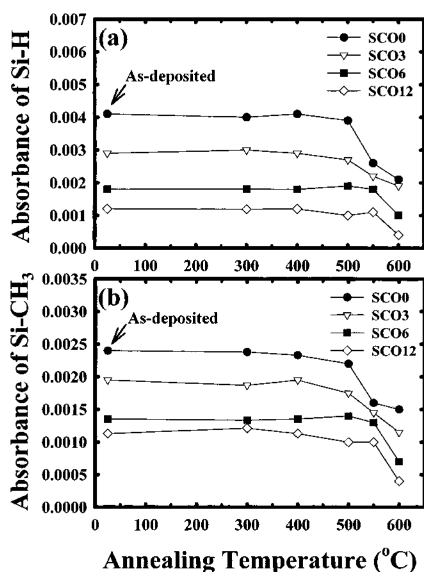

Figure 2. Annealing temperature dependence of FTIR absorbance peak height for (a) Si-H (2100 cm^{-1}) absorbance and (b) Si-CH_3 (1250 cm^{-1}) absorbance for 3MS-based α-SiC(O) dielectric films.

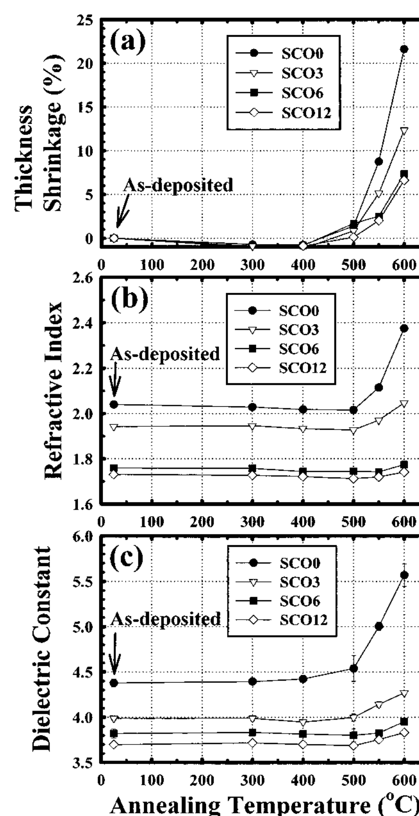

Figure 3. (a) Thickness shrinkage, (b) refractive index, and (c) dielectric constant *vs.* annealing temperature for 3MS-based α-SiC(O) dielectric films.

Downloaded on 2014-04-27 to IP 140.113.38.11 address. Redistribution subject to ECS terms of use (see ecsdl.org/site/terms_use) unless CC License in place (see abstract).

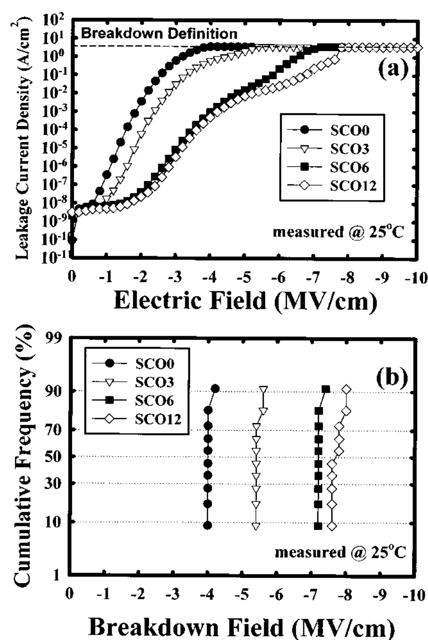

Figure 4. (a) Leakage current density *vs.* electric field and (b) statistical distribution of breakdown field for the 400°C annealed Al-gated MIS capacitors.

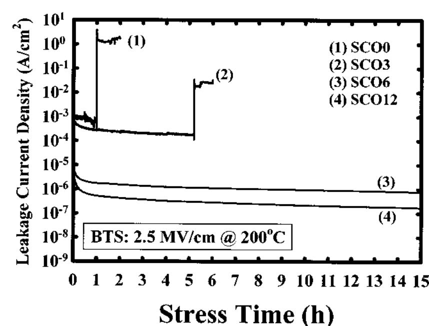

Figure 6. Current transient during BTS test at 200°C with an electric field of 2.5 MV/cm for the 400°C annealed TaN/Cu-gated MIS capacitors.

electric barriers. For each dielectric barrier, negligible difference in leakage current was observed between the as-fabricated and the 400°C annealed MIS capacitors. This implies that all the dielectric barriers are capable of preventing Cu penetration at temperatures up to 400°C. The fact that the breakdown field and the leakage current density of the α-SiC(O) dielectric films depend on the CO_2 flow rate (Fig. 4b and 5b) might be due to the denser and less porous film structure (Table II). BTS test was used to further explore the dielectric barrier property of the α-SiC(O) films. In these tests, the TaN/Cu MIS capacitor structure annealed at 400°C was used. The BTS test was performed at 200°C with an applied electric field of 2.5 MV/cm on the MIS capacitors. N_2 purging was used to prevent the oxidation of the Cu electrode and moisture uptake in the dielectric barriers during the BTS test. Figure 6 shows the leakage current transient during the BTS test. Current-spiking occurred for the SCO0 and SCO3 dielectric MIS samples after 1 and 5 h, respectively, whereas the SCO6 and SCO12 dielectric MIS samples remained stable up to at least 15 h. Figure 7 shows the instantaneous leakage current density *vs.* the applied electric field (in accumulation mode) before and after the BTS for the MIS capacitors. Significant leakage current increase was detected for the TaN/Cu MIS capacitors made from SCO0 and SCO3 films after 2 and 6 h BTS, respectively. Figure 8 shows the time-to-breakdown, under different BTS conditions, for the 400°C-annealed TaN/Cu MIS capacitors with α-SiC(O) dielectric deposited with various CO_2 flow rates. All BTS tests were stopped at 15 h, and all the 400°C annealed Al MIS capacitors with α-SiC(O) dielectrics remained stable up to at least 15 h under the BTS of 3 MV/cm at 200°C (not shown). This further confirms that the current-spiking during the BTS test (Fig. 6) and the significant leakage current increase after the BTS test (Fig. 7) in the 400°C annealed TaN/Cu MIS capacitors made from SCO0 and SCO3 films are due to the penetration of Cu into the dielectric barriers rather than the BTS-induced dielectric breakdown. The improved barrier properties of the α-SiC(O) dielectric films deposited with high CO_2 flow rates is attributed to the denser and more crosslinked film structure; thus, the Cu ions may be less mobile in the dense film.[16,19-23] However, the Cu barrier properties of the α-SiC(O) dielectric films degrade with high O_2 flow rates.[9] Because abundant oxygen in dielectric films will possibly enhance the penetration of Cu into the dielectric film by Cu-O reactions,[10,24] ability for the film to prevent Cu diffusion is expected to degrade with higher flow rates of oxygen-containing gas during the film's deposition process.[9,10]

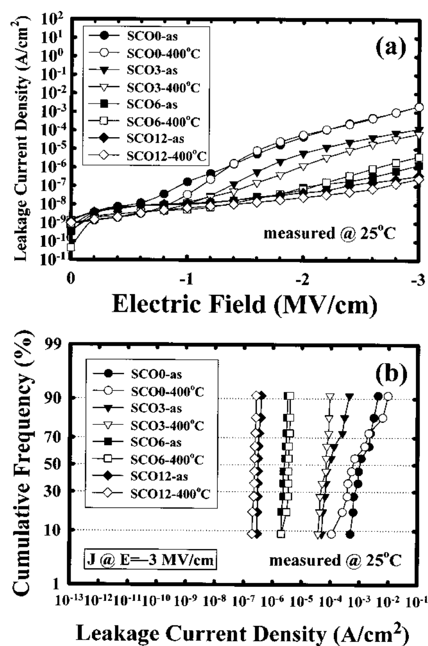

Figure 5. (a) Leakage current density *vs.* electric field and (b) statistical distribution of leakage current density at an applied electric field of 3 MV/cm for the as-fabricated and 400°C annealed TaN/Cu-gated MIS capacitors.

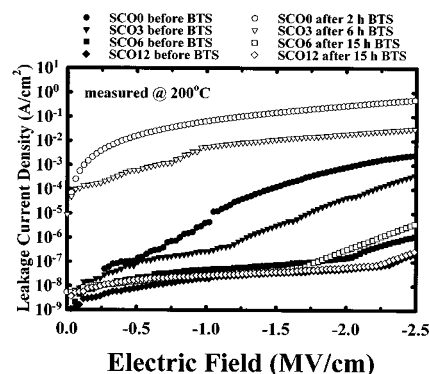

Figure 7. Instantaneous leakage current density *vs.* applied electric field before and after the BTS (2.5 MV/cm at 200°C) for the TaN/Cu MIS capacitors with SCO0, SCO3, SCO6, and SCO12 dielectric films.

Downloaded on 2014-04-27 to IP 140.113.38.11 address. Redistribution subject to ECS terms of use (see ecsdl.org/site/terms_use) unless CC License in place (see abstract).

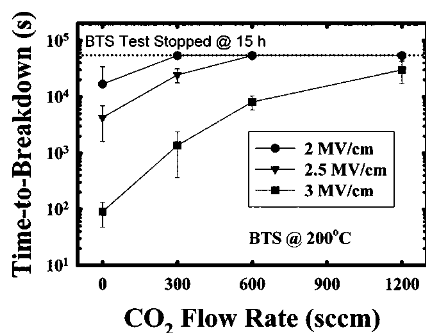

Figure 8. Time-to-breakdown under different BTS conditions for the 400°C annealed TaN/Cu MIS capacitors with α-SiC(O) dielectric films deposited with various CO_2 flow rates.

However, the α-SiCO film deposited in this work using PECVD at 1200 sccm CO_2 flow rate still exhibits a superb barrier property. This might be due to the fact that the SCO12 film's chemical composition is SiC-based rather than SiO-based (Table II).

Conclusion

Four α-SiC(O) films were deposited using PECVD from 3MS precursor without and with three different CO_2 flow rates. The resulting films were investigated with respect to their thermal stability and physical and barrier properties. With the addition of CO_2 during the dielectric deposition process, the dielectric constant of the α-SiCO dielectric films decreases with increasing CO_2 flow rate. Increasing CO_2 flow rate also promotes better thermal stability, higher breakdown field, lower leakage current, and superior resistance to Cu diffusion. The improved barrier property is attributed to the denser and less porous structure of the α-SiCO dielectric barrier. The α-SiCO dielectric barrier deposited with the large (1200 sccm) CO_2 flow rate exhibits the low k value of 3.7, thermal stability up to 550°C, room-temperature breakdown field of 8 MV/cm and leakage current densities of 10^{-7} to 10^{-6} A/cm^2 at 3 MV/cm, and a superb Cu barrier property.

Acknowledgments

The authors express their gratitude to Professor Bing-Yue Tsui of National Chiao-Tung University for his helpful discussion.

National Chiao-Tung University assisted in meeting the publication costs of this article.

References

1. F. Lanckmans, W. D. Gray, B. Brijs, and K. Maex, *Microelectron. Eng.,* **55**, 329 (2001).
2. J. Martin, S. Filipiak, T. Stephens, F. Huang, M. Aminpur, J. Mueller, E. Demircan, L. Zhao, J. Werking, C. Goldberg, S. Park, T. Sparks, and C. Esber, *Proc. IEEE,* **IITC**, 42 (2002).
3. S. G. Lee, Y. J. Kim, S. P. Lee, H. Y. Oh, S. J. Lee, M. Kim, I. G. Kim, J. H. Kim, H. J. Shin, J. G. Hong, H. D. Lee, and H. K. Kang, *Jpn. J. Appl. Phys., Part 1,* **40**, 2663 (2001).
4. C. C. Chiang, M. C. Chen, Z. C. Wu, L. J. Li, S. M. Jang, C. H. Yu, and M. S. Liang, *Proc. IEEE,* **IITC**, 200 (2002).
5. C. C. Chiang, I. H. Ko, M. C. Chen, Z. C. Wu, Y. C. Lu, S. M. Jang, and M. S. Liang, *Proc. IEEE,* **IITC**, 201 (2003).
6. K. Goto, H. Yuasa, A. Andatsu, and M. Matsuura, *Proc. IEEE,* **IITC**, 6 (2003).
7. T. Ishimaru, Y. Shioya, H. Ikakura, M. Nozawa, Y. Nishimoto, S. Ohgawara, and K. Maeda, *Proc. IEEE,* **IITC**, 36 (2001).
8. K. I. Takeda, D. Ryuzaki, T. Mine, and K. Hinode, *Proc. IEEE,* **IITC**, 244 (2001).
9. Y. W. Koh, K. P. Loh, L. Rong, A. T. S. Wee, L. Huang, and J. Sudijono, *J. Appl. Phys.,* **93**, 1241 (2003).
10. T. Ishimaru, Y. Shioya, H. Ikakura, M. Nozawa, S. Ohgawara, T. Ohdaira, R. Suzuki, and K. Maeda, *J. Electrochem. Soc.,* **150**, F83 (2003).
11. A. Grill and V. Patel, *J. Appl. Phys.,* **85**, 3314 (1999).
12. L. M. Han, J. S. Pan, S. M. Chen, N. Balasubramanian, J. Shi, L. S. Wong, and P. D. Foo, *J. Electrochem. Soc.,* **148**, F148 (2001).
13. C. Kittel, *Introduction to Solid State Physics*, 7th ed., p. 390, John Wiley & Sons, New York (1996).
14. S. M. Han and E. S. Aydil, *J. Appl. Phys.,* **83**, 2172 (1998).
15. J. Y. Kim, M. S. Hwang, Y. H. Kim, H. J. Kim, and Y. Lee, *J. Appl. Phys.,* **90**, 2469 (2001).
16. Z. C. Wu, Z. W. Shiung, C. C. Chiang, W. H. Wu, M. C. Chen, S. M. Jeng, W. Chang, P. F. Chou, S. M. Jang, C. H. Yu, and M. S. Liang, *J. Electrochem. Soc.,* **148**, F127 (2001).
17. C. C. Chiang, M. C. Chen, C. C. Ko, Z. C. Wu, S. M. Jang, and M. S. Liang, *Jpn. J. Appl. Phys., Part 1,* **42**, 4273 (2003).
18. C. C. Chiang, Z. C. Wu, W. H. Wu, M. C. Chen, C. C. Ko, H. P. Chen, S. M. Jang, C. H. Yu, and M. S. Liang, *Jpn. J. Appl. Phys., Part 1,* **42**, 4489 (2003).
19. A. L. S. Loke, J. T. Wetzel, P. H. Townsend, T. Tanabe, R. N. Vrtis, M. P. Zussman, D. Kumar, C. Ryu, and S. S. Wong, *IEEE Trans. Electron Devices,* **46**, 2178 (1999).
20. D. Gupta, *Mater. Chem. Phys.,* **41**, 199 (1995).
21. J. D. Mcbrayer, R. M. Swanson, and T. W. Sigmon, *J. Electrochem. Soc.,* **133**, 1242 (1986).
22. J. L. Duda and N. Faridi, in *Diffusion in Amorphous Materials*, H. Jain and D. Gupta, Editors, p. 55, TMS, Warrendale, PA (1994).
23. D. Gupta, F. Faupel, and R. Willecke, in *Diffusion in Amorphous Materials*, H. Jain and D. Gupta, Editors, p. 189, TMS, Warrendale, PA (1994).
24. Y. S. Diamand, A. Dedhia, D. Hoffstetter, and W. G. Oldham, *J. Electrochem. Soc.,* **140**, 2427 (1993).

Downloaded on 2014-04-27 to IP 140.113.38.11 address. Redistribution subject to ECS terms of use (see ecsdl.org/site/terms_use) unless CC License in place (see abstract).